MAGNETIC RESONANCE IN CHEMISTRY
Magn. Reson. Chem. **36**, 913–920 (1998)

Analysis of NMR data and global fold of the [Fe_4–S_4] ferredoxin I from *Desulfovibrio desulfuricans* Norway

Evelyne Lebrun*

Bioénergétique et Ingénierie des Protéines, CNRS, 31 chemin Joseph Aiguier, 13402 Marseille Cedex 20, France

Received 20 April 1998; revised 25 June 1998; accepted 13 July 1998

ABSTRACT: The oxidized form of the [Fe_4–S_4] ferredoxin I from *Desulfovibrio desulfuricans* Norway (*Dd*N Fd I) was investigated by ^{1}H and ^{13}C NMR spectroscopy. The sequence-specific ^{1}H assignments of 93% of the amino acid residues of the whole protein, a complete determination of its secondary structure and an identification of a disulfide bridge are reported. The secondary structure of *Dd*N Fd I was determined from both sequential and spatial NOEs. These NOEs reveal two anti-parallel β-sheets including Thr1–Ile4 and Glu59–Ile56, Val22–Ile26 and Thr35–Lys31, one helical segment (ranging from Ala41 to Asp49) and three tight turns. Three-dimensional features of *Dd*N Fd I were evidenced from long-range NOE cross peaks between the secondary structural elements of the protein. Among them, a possible disulfide bridge, located between the pair of cysteines which are not coordinated to the cluster, was indicated by a ^{13}C–^{1}H HSQC experiment at natural abundance. The comparison of secondary structural elements and tertiary contacts of *Dd*N Fd I protein with those of ferredoxins from mesophilic bacteria *Desulfovibrio gigas* and *Desulfovibrio africanus* and that from the hyperthermostable archaeon *Thermococcus litoralis* confirms that *Dd*N Fd I exhibits the same global protein folding topology as the others. The chemical shifts of *Dd*N Fd I were compared with those of other monocluster-type ferredoxins. They show a peculiar conservation of the hydrophobic core of these ferredoxins. © 1998 John Wiley & Sons, Ltd.

KEYWORDS: NMR; ^{1}H NMR; metalloproteins; iron–sulfur cluster; disulphide bridge; *Desulfovibrio desulfuricans* Norway; ferredoxin I

INTRODUCTION

Iron–sulfur proteins are widely distributed in nature.[1] Iron–sulfur proteins are ubiquitous electron transport proteins, which perform a large variety of chemical reactions from steroid hydroxylation, CO_2 and H_2 fixation to oxidative phosphorylation and photosynthesis. Such specific electronic transfers are processed via inorganic moieties, the Fe/S centers, bound to cysteines.[2] Several studies[3–6] have led to progress in the knowledge of the electron transfer and regulation of the redox potential of these proteins.

Bacterial ferredoxins[7] are the simplest iron–sulfur proteins. Most of them have one or two ([Fe_4–S_4] or [Fe_3–S_4]) clusters per molecule and among them several atomic structures are available from x-ray diffraction studies[8–15] and NMR data.[16–21] The low-potential ferredoxins exhibit a wide range of redox potential, ranging from -150 to -645 mV. However, no clear structural parameter can account for the differences observed with respect to redox midpoint potentials. In addition to x-ray studies, ferredoxins have also been the subject of numerous spectroscopic investigations by means of Mössbauer, EPR and ENDOR techniques.[1,22] More recently, appropriate 2D NMR methodology[14–26] allowed the sequence-specific assignments of the amino acid residues close to the paramagnetic centers.[5–34]

The ferredoxin *Dd*N Fd I was purified from the sulfate-reducing bacterium *Desulfovibrio desulfuricans* strain Norway. This ferredoxin is a small iron–sulfur protein of 59 amino acids containing a single [Fe_4–S_4] cluster which presents two redox states ([Fe_4–S_4]$^{2+}$ and [Fe_4–S_4]$^{+}$) with a redox potential of -375 mV. *Dd*N Fd I shows high sequence similarities to ferredoxins from mesophilic bacteria such as 3Fe *Desulfovibrio gigas* (*Dg* Fd II) and 4Fe *Desulfovibrio africanus* (*Da* Fd I) with amino acid identities of 46 and 41%, respectively, and, at a lesser extent (37%), with the hyperthermostable 4Fe *Thermococcus litoralis* ferredoxin (*Tl* Fd).

X-ray structures of both *Dg* Fd II[12] and *Da* Fd I[13] are known at 1.7 and 2.3 Å resolution, respectively. A molecular model of the solution structure for the 4Fe *Tl* Fd was proposed by Wang *et al.*[35] The x-ray structure of the oxidized 3Fe form of the single-cluster *Dg* Fd II[12] revealed the existence of a disulfide bridge between the two cysteines that remain from the consensus sequence of deleted cluster 2. Such a disulfide bridge was found again in oxidized 3Fe *Pyrococcus furiosus* ferredoxin (*Pf* Fd);[36] it was suggested that the disulfide bridge might represent another supplementary way for electron transport.

NMR characterization of the *Dd*N Fd I molecule was initiated with the aim of gaining some insight into the structural relationship between this ferredoxin and its biological partners. A preliminary NMR study,[37]

* *Correspondence to*: E. Lebrun, Bioénergétique et Ingénierie des Protéines, CNRS, 31 chemin Joseph Aiguier, 13402 Marseilles Cedex 20, France. E-mail: lebrun@ibsm.cnrs-mrs.fr

CCC 0749-1581/98/120913–08 $17.50

oriented towards the detection of the slowly relaxing protons (i.e. in the diamagnetic region), has already shown the presence of an α-helix in the protein. In a previous paper,[33] we presented the ^{1}H NMR spectral properties of the cluster-ligated Cys in both redox states of *Dd*N Fd I.

We report here the sequence-specific ^{1}H NMR assignments for *Dd*N Fd I and the secondary structure derived from NOEs between different backbone protons and from observations of slowed exchange of hydrogen-bonded amide protons with the solvent. The spatial relationship between secondary structural elements of *Dd*N Fd 1 is evidenced and compared with those of other mesophilic (*Desulfovibrio* type) and hyperthermostable (*Archaea* type) ferredoxins. Cross-peak NOEs for residues near Cys19 and Cys43 suggest the existence of a disulfide bridge in the oxidized form of *Dd*N Fd I.

EXPERIMENTAL

Sample preparation

*Dd*N Fd I was purified as reported previously.[38] NMR samples were prepared in 0.1 M potassium phosphate buffer (pH 5.9). Two samples were used, one in 90% H_2O–10% D_2O at a protein concentration of 5.0 mM and the other in D_2O (final concentration 2.3 mM, after five solvent exchanges on an Amicon Centricon micro-concentrator.

NMR spectroscopy

NMR experiments of the *Dd*N Fd I were recorded on a Bruker Avance DRX 500 spectrometer. The experiments were performed at 283 and 298 K. ^{1}H chemical shifts were referenced to the water signal resonance set to 4.78 ppm at 298 K. Generally, spectra were recorded with a spectral width of 6000 Hz.

At 283 and 298 K, TOCSY [512 (t_1) × 2048 (t_2)] complex data points and NOESY (4096 × 512) were acquired in either H_2O or D_2O. TOCSY experiments were performed with quadrature detection in both dimensions using an MLEV-17 scheme.[39] The spin lock times were 60 and 80 ms. When needed, the water peak was eliminated by presaturation during the appropriate delays.

Phase-sensitive DQF COSY [512 (t_1) × 4096 (t_2)] complex data points with presaturation during relaxation delay were acquired at 298 K in H_2O.[40]

Phase-sensitive two-dimensional nuclear Overhauser effect spectra (NOESY)[41] with watergate composite were acquired using TPPI with mixing times of 100, 150 and 300 ms.

The ^{13}C–^{1}H correlation spectrum was recorded at 298 K, at natural abundance (protein concentration 5 mM) using the HSQC pulse sequence.[42,43] The HSQC was collected into 2048 complex data points in the t_2 dimension and 256 complex data points in the t_1 dimension with 800 scans per t_1 experiment. The spectral widths were 6009.6 and 12 576.2 Hz in F_2 and F_1, respectively. ^{13}C decoupling during acquisition was achieved using the GARP sequence.[44] Carbon chemical shifts were calibrated by setting the zero point of the ^{13}C frequency scale equal to 0.251 450 02 times the proton zero frequency.

All 2D data processing was performed on a Silicon Graphics workstation using the MSI FELIX 95.0 software package (Hare Research) including the semi-automatic assignment procedure (ASSIGN).

The t_1 dimension was zero-filled to 2048 real data points with both dimensions being multiplied by a sine-bell function shifted by 90° before Fourier transformation. A fifth-order polynomial baseline correction was used to improve the appearance of the spectra.

NOE cross-peak intensities were measured using the integration function within MSI FELIX 95.0. The calibration curve was based on the $d_{\alpha N}$ cross-peaks, which correspond to a known distance ($d_{\alpha N}$ β-sheet = 2.2 Å[45]) and classified as strong, medium and weak, corresponding to 1.8–2.7, 1.8–3.5 and 1.8–5.0 Å, respectively.[46]

Molecular modeling

As spin systems are often incomplete, owing to paramagnetic effects, a structural model was used in the previous ^{1}H NMR study[33] as a guide for assignments of the protons belonging to the cluster-ligated cysteines. Such an essential tool was used again in the present study to support the assignments of a few other fast-relaxing protons lying at short distances from the cluster.

The initial 3D model for *Dd*N Fd I was generated, using a set of coordinates obtained from the x-ray structure of *Dg* Fd II[12] (a closely related but [Fe_3–S_4] cluster ferredoxin), by substituting amino acids when needed and by inserting the [Fe_4–S_4] center of the monocluster ferredoxin from *Bacillus thermoproteolyticus* (*Bt* Fd).[10] The molecular modeling was performed using the computer software packages HOMOLOGY, INSIGHT II and DISCOVER from MSI.

The refinement[33] of the initial structure of *Dd*N Fd I was performed with X-Plor[47] using the topology and parameters files tophopls.pro and parhopls.pro derived from AMBER plus additional parameters for the iron–sulfur site.[48] During the process of refinement, the geometry of the cluster was preserved.

The atomic coordinates of the x-ray structures of *Dg* Fd II, *Da* Fd I and *Bt* Fd were used to calculate the water access surface by residue for each ferredoxin. The algorithm used is from Kabsch and Sander's[49] DSSP program (TURBO-FRODO).

RESULTS AND DISCUSSION

Sequence-specific assignments of ^{1}H resonances

Sequence-specific assignments of the residues, in the diamagnetic region, were achieved following the method

descried by Wüthrich.[45] Forty-one backbone amide resonances were correlated with side-chain spin systems by DQF COSY and TOCSY recorded in H_2O at 283 and 298 K. Some spin systems not resolved were recognized from analogous experiments carried out in D_2O.

All pro residues (Pro20, Pro37 and Pro52) were identified by the TOCSY lines starting from their $\delta\delta'$ protons to their αH proton; their connectivities were established by the α_i–$\delta\delta'_{i+1}$ and α_i–N_{i+1} medium NOE cross peaks: αHCys19–$\delta\delta'$HPro20, αHAla36–$\delta\delta'$HPro37 and αHPro52–HNVal53. Sequential assignments of the other amino acid residues were made by the sequential $\delta\alpha N(i, i+1)$ and $\delta NN(i, i+1)$ connectivities. The NH–NH region of a NOESY spectrum (150 ms) in H_2O is shown in Fig. 1. This spectrum illustrates the characteristic sequential assignments of helix segments. Figure 3(A) provides a summary of the sequential and medium-range NOEs observed for the *Dd*N Fd I.

A previous study[33] with NMR experiments tailored to the detection of fast-relaxing resonances led to the complete assignments of the cysteines [Cys9 (**I**), Cys12 (**II**), Cys15 (**III**) and Cys51 (**IV**) ligating the cluster. These experiments also permitted the sequential assignments of other residues located in the proximity of the cluster (Leu18, Phe23 and Ala47), which exhibit NOE cross peaks with Cys15 (**III**). Val22 was unambiguously identified because of its NOEs towards aromatic protons of Phe23 and also the characteristic upfield peak of one of its γ-CH_3 group. Such an anisotropic shield effect was observed previously as a unique feature in the spectra of *Pf* and *Tl* ferredoxins. The spin system assigned to Ib4, Val16, Ala32 and Ib56 were only observed in TOCSY with short spin-lock (range 4–15 ms) and NOESY with mixing times of 10 and 20 ms.[33] The spin system of I10 was assigned by exclusion.

The use of a model of the protein structure was helpful in correlating data obtained from TOCSY experiments, with short and long mixing times. Nevertheless, all the spin systems expected for *Dd*N Fd I were not fully observed. Among the 59 spin systems of the ferredoxin, four spin systems were completely missing: those of Gly11, Glu13, Ser14 and Ala55. However, the protein model predicts all these four residues to be in the close vicinity of the cluster, resulting in very large broadening of the respective resonance lines due to paramagnetic effects.[23] The sequence-specific assignments of ^1H resonances resulting from these spectra are summarized in Table 1.

Analysis of the ^{13}C ^1H correlation spectrum of the *Dd*N Fd I

The ^{13}C–^1H correlation spectrum of the *Dd*N Fd I (Fig. 2) was recorded at natural abundance in order to corroborate the existence of a disulfide bridge. The assignment of the ^{13}C spectrum was greatly assisted by the availability of ^1H resonance assignments of *Dd*N Fd I. Most of the protons attached to the same carbon were unambiguously identified (complete results not shown here). Figure 2 shows an expansion of the area of interest (i.e. the $\beta\beta'$ chemical shift region of cysteines) in the ^{13}C–^1H correlation (HSQC) spectrum of *Dd*N Fd I. Two $\beta\beta'$HCys19 and two $\beta\beta'$HCys43 protons previously assigned at 3.41/2.64 ppm and 3.80/2.91 ppm

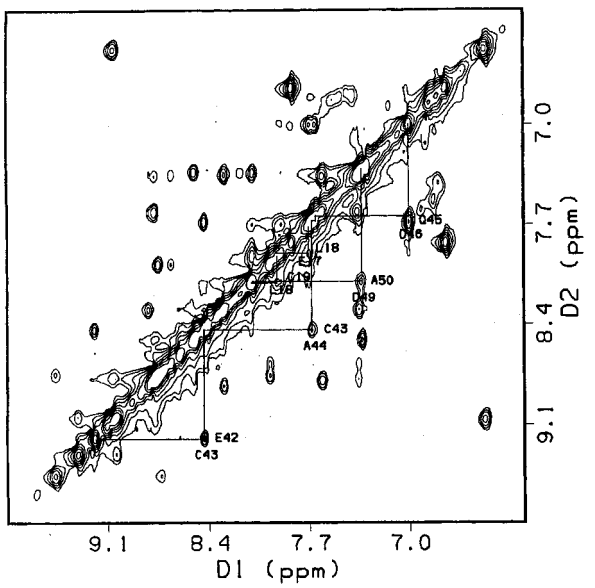

Figure 1. NH region of a 150 ms NOESY NMR spectrum of *Dd*N Fd I [H_2O–D_2O (90:10), 298 K] showing the sequential NH_i to NH_{i+1} connectivities between residues 17 to 19 and 42 to 50.

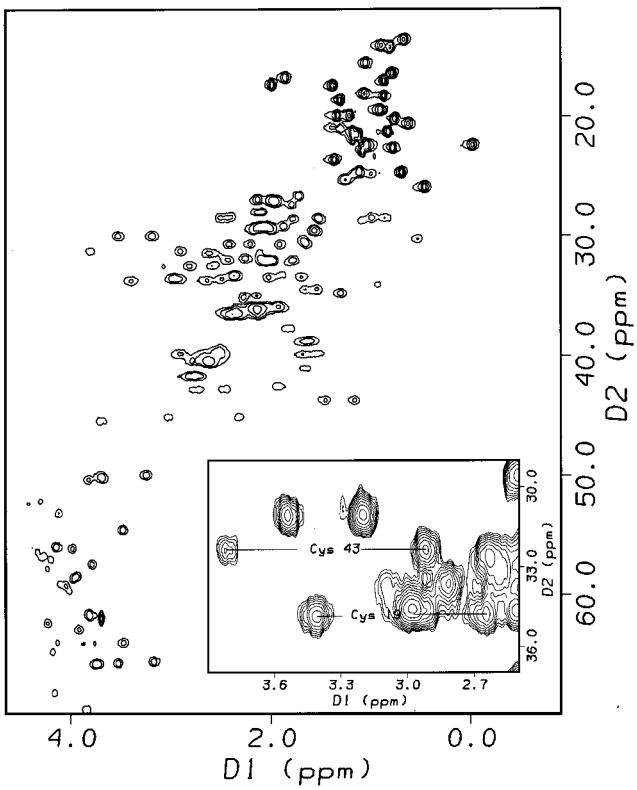

Figure 2. ^{13}C–^1H HSQC spectrum of the oxidized *Dd*N Fd I. The inset shows the $\beta\beta'$ chemical shifts region of cysteines. The $^{13}C_\beta$ of Cys19 and Cys43 chemical shift values are 34.6 and 32.2 ppm, respectively.

Table 1. Sequence-specific assignments of the protons of the oxidized form of *D. desulfuricans* Norway ferredoxin I in H_2O at pH 5.9 and 298 K

Residue	NH	H_α	H_β	H_γ	H_δ	Others
Thr 1		4.17	3.83	1.16		
Ile 2	9.11	4.69	1.78	1.60/1.18/0.84	0.82	
Val 3	9.05	4.56	1.92	0.83/0.77		
Ile 4	8.61	4.94	1.92	1.26/1.03/0.87	0.68	
Asp 5	8.89	4.69	2.50/2.93			
His 6	8.44	4.72	2.75/2.91			8.70/7.35
Glu 7	8.65	4.42	1.98	2.19		
Glu 8	8.51	4.43	2.11	2.63/2.79		
Cys 9		4.11	β_1/β_2 11.25/7.57			
Ile10	8.94	4.65	1.79	1.58/1.11/0.81	0.75	
Gly11						
Cys12		10.51	$\beta_1\beta_2$ 10.2/16.87			
Glu13						
Ser14						
Cys15		7.14	β_1/β_2 16.08/4.57			
Val16	6.67	3.53	2.31	1.14		
Glu17	7.73	3.98	2.02/2.11	2.26/2.38		
Leu18	7.92	4.15	1.45/1.17	1.73	0.77/0.46	
Cys19	8.11	5.49	3.41/2.64			
Pro20	—	5.09	2.64/2.15	2.03/2.00	3.68/3.81	
Glu21	8.78	4.24	1.98/1.79	2.11		
Val22	7.62	3.93	1.29	0.69/ − 0.02		
Phe23	7.38	5.54	3.04/2.33			6.86/6.82
Ala24	8.74	4.68	1.36			
Met25	8.76	5.33	2.01/2.15	2.56/2.81		
Ile26	8.77	3.81	1.69	1.56/1.06/0.65	0.87	
Asp27	8.51	4.41	2.52/2.79			
Gly28	8.76	3.71/3.73				
Glu29	7.98	4.62	1.71/1.87	2.03/2.15		
Glu30	8.67	4.41	1.80/1.95	2.16		
Lys31	8.32	5.26	1.53			2.74/2.37
Ala32	7.55	5.71	2.21			
Met33	9.47	5.04	2.16/1.94	2.42/2.22		
Val34	8.43	4.42	2.65	0.90/0.86		
Thr35	9.07	4.24	3.86	1.04		
Ala36	6.48	5.05	1.32			
Pro37	—	4.19	2.64/2.44	1.98/2.07	3.24/3.70	
Asp38	8.52	4.91	2.64/2.54			
Ser39	8.78	4.19	3.73			
Thr40	8.75	4.42	4.16	1.07		
Ala41	8.61	4.13	1.31			
Glu42	9.19	4.07	2.04/2.08	2.42		
Cys43	8.44	4.72	3.80/2.91			
Ala44	7.69	3.99	1.37			
Gln45	7.68	3.79	2.09	2.36		6.74/7.82
Asp46	6.99	4.19	2.56/2.67			
Ala47	7.71	3.49	0.91			
Ile48	7.89	3.18	1.84	1.69/0.53/0.67	0.78	
Asp49	8.09	4.34	2.64			
Ala50	7.34	4.14	1.33			
Cys51	7.29	4.35	$\beta_1\beta_2$ 6.26/11.69			
Pro52	—	4.03	2.43/2.30	2.02	3.22/3.58	
Val53	8.81	4.41	2.09	1.02/0.63		
Glu54	8.31	3.94	2.05/2.17	2.37		
Ala55						
Ile56	7.33	5.19	1.91	1.67/0.91		
Ser57	9.32	4.66	3.74			
Lys58	8.35	5.16	1.66/1.54	1.26	0.91	3.22/2.77/7.29
Glu59	8.72	4.27	1.88/1.78	2.05		

were correlated with the $^{13}C_{\beta}$Cys19 and $^{13}C_{\beta}$Cys43 at 34.6 and 32.2 ppm, respectively.

Secondary structure

The elements of secondary structure shown in *Dd*N Fd I consist of one α-helix (αB), two β-sheets (βA and βB) and three tight turns (B, C and E) (Fig. 3).

The α-helix B (αB) is evidenced by eight $d_{NN(i,i+1)}$ NOEs: they form a continuous set ranging from Ala41 to Asp49 [Figs 1 and 3(A)]. Such a secondary structural element is also found in other monocluster ferredoxins within equivalent positions. This α-helix B has the same length in *Dd*N Fd I, *Dg* Fd II and *Tl* Fd [see Fig. 3(A), (C) and (D)] but it is three residues longer in *Pf* Fd and *Da* Fd. In addition, two medium-range NOEs, αHVal16–NHCys19 and αHGlu17–NHCys19 [Fig. 3(A)] were observed in *Dd*N Fd I; they suggest the presence of a helical segment, such as the short one (αA) found, at equivalent positions, in *Dg* Fd II and *Tl* Fd [Fig. 3(C) and (D)]. This short α-helix A was not fully observed in *Dd*N Fd I because of a close proximity to the cluster.

The β-sheet B (βB) was identified by inter-strand NOE interactions arising from protons involved in the short αH_i–αH_j distances. A first pattern involves αHPhe23–αHVal34 and includes NOEs to the $i+1$ and $j+1$ amide NHs (αHPhe23–NHAla24 and αHVal34–NHThr35) describing a trapezoid shape which characterizes an anti-parallel β-sheet [Fig. 4(B)]. A second pattern involves αHMet25–αHAla32, αHMet25–NHIle26 and αHAla32–NHMet33. These patterns are characteristic of an anti-parallel β-strand (βB) in the inner core of the protein.

The β-sheet A (βA) formed by the N- and C-termini of the protein was identified by four inter-strand NOE interactions that involve αHIle2–αHLys58, αHLys58–NHVal3, αHIle4–NHSer57 and NHVal3–NHSer57 NOEs [see Fig. 4(A)]. The small number of NOESY cross peaks observed in the β-sheet A is due to near degeneracy because of the proximity of the [4Fe–4S] cluster. Therefore, an αHIle4–αHIle56 NOESY cross peak is not detected. These data confirm the existence of a short anti-parallel β-strand (βA) consisting of amino acids Thr1–Ile4 and Glu59–Ile56. It is of interest to note that the double-stranded β-sheet A found in *Dd*N Fd I corresponds to the structural element found in *Dg* Fd II [Fig. 3(C)] rather than to the triple-stranded one [Fig. 3(D)] observed in the hyperthermostable ferredoxin from *Tl* Fd[19] and *Pf* Fd.[20]

Analysis of the NMR experiments made with the D_2O sample reveals the location of the hydrogen-bonded amide protons. This analysis confirms both β-sheet structures found in *Dd*N Fd I; the protons involved in hydrogen bonds are indicated by circles in Fig. 4(A) (β-sheet A) and in 4(B) (β-sheet B).

The presence of α-helical and β-sheet structures can

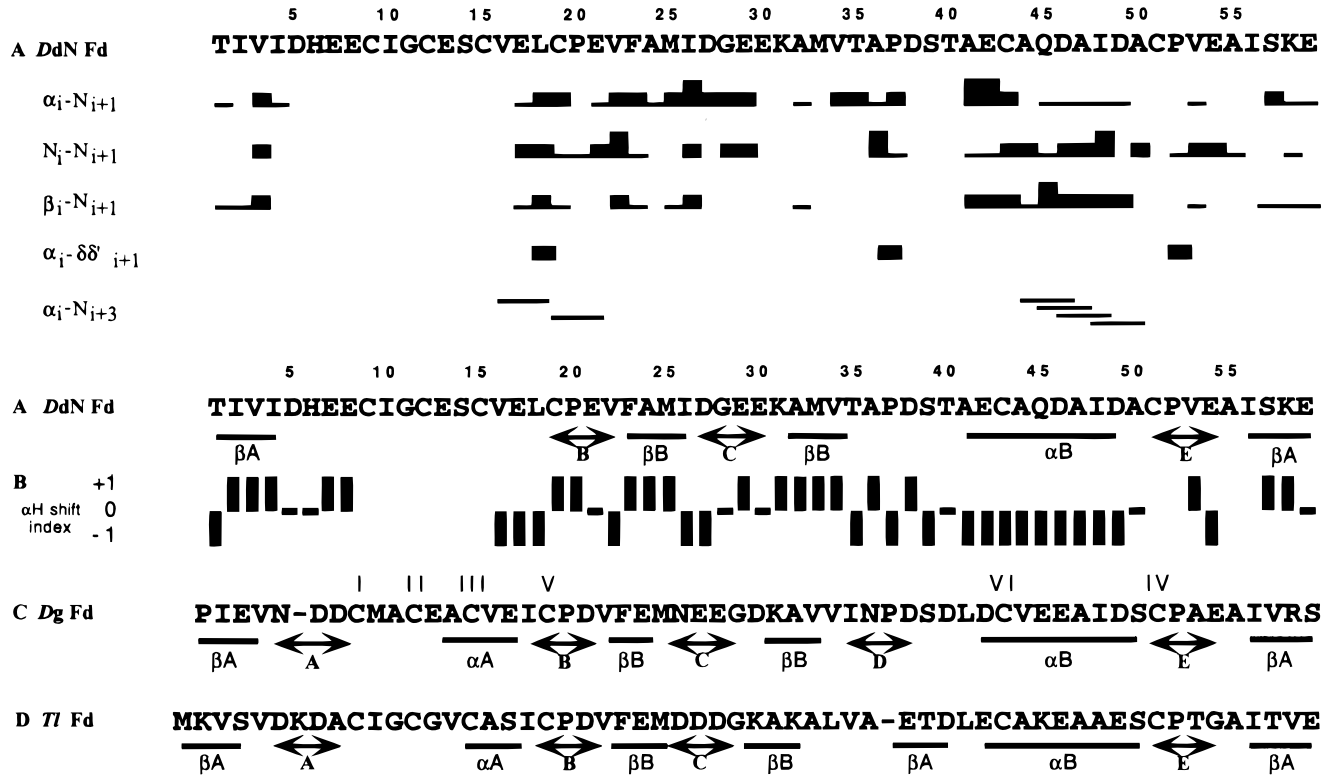

Figure 3. Sequences and secondary structure elements of *Dd*N Fd I (A), *Dg* Fd II and *Tl* Fd I (C, D). Summary of NOE information obtained for the *Dd*N Fd I in H_2O–D_2O (90 : 10) at pH 5.9. The thickness of the lines indicates the intensities of the NOE cross peaks, which are strong, medium and weak. (B) αH shift index data for *Dd*N Fd I providing an indication of secondary structure.

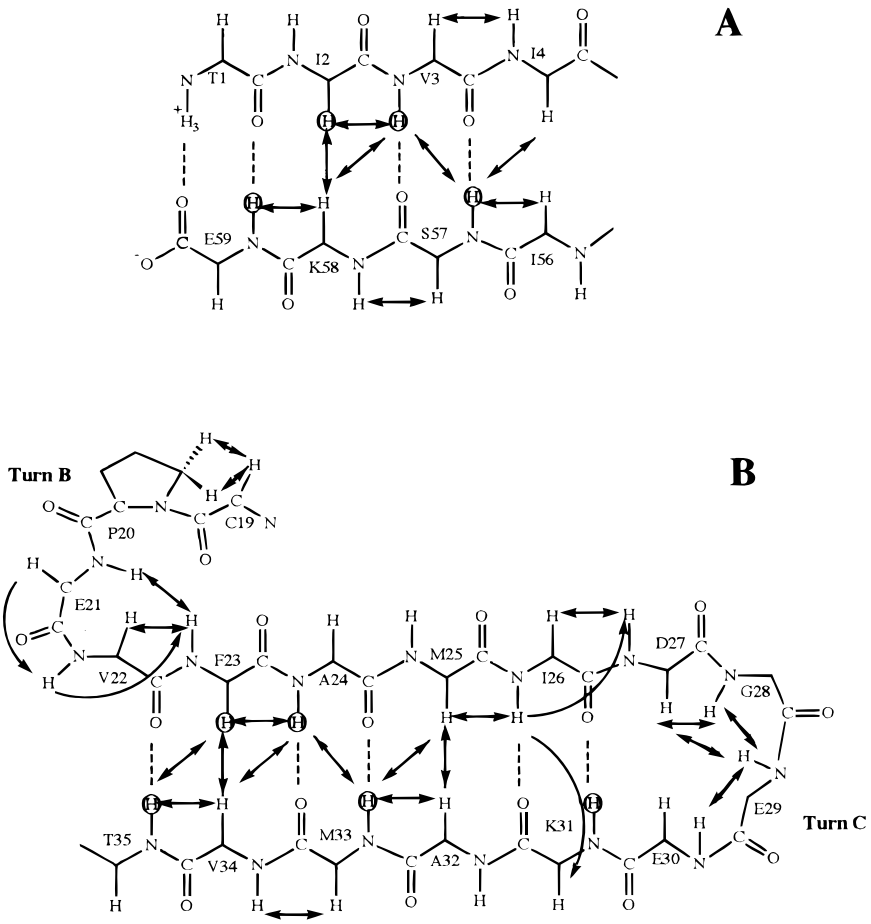

Figure 4. Representation of the β-sheet secondary structures in *Dd*N Fd I: (A) β-sheet A; (B) β-sheet B. The pattern of observed NOEs is indicated by double-headed arrows. The presence of the inter-strand hydrogen bonds is shown by dashed lines. The slowly exchanging backbone amide protons are marked by circles.

be confirmed by the observation of secondary chemical shift indexes[50] of the α-protons in *Dd*N Fd I [Fig. 3(B)]. The sudden changes in the chemical shift index involving residues 18–20, 26–29 and 52–54 are indicative of β-turns which are conserved in other ferredoxins.

Three tight turns (B, C and E) are described in Fig. 3(A). The β-turn B is well defined by medium, strong and medium NHGlu21–NHVal22, NHVal22–NHPhe23 and NHGlu21–NHPhe23 NOEs, respectively [Figs 3(A) and 4(B)]. The β-turn C also is confirmed by two medium NOEs, NHGly28–NHGlu29 and NHGlu29–NHGlu30, as illustrated in Figs 3(A) and 4(B). The β-turn E, present just after Cys 51 (**IV**) in *Dg* Fd II, is also well defined in *Dd*N Fd I by an NHVal53–NHGlu54 NOE cross peak [Fig. 3(A)]. Moreover, in the NOESY spectra with short mixing times (10 and 20 ms) in D_2O, the $C_{\beta 1}H$ of Cys51 exhibits two NOE cross peaks, with resonances at 3.98 and 8.30 ppm, which belong to αH and NH of Glu54, respectively.[33]

The β-turns B and C appear to be conserved in the monocluster-type ferredoxins. The β-turn A (found in *Dg* Fd II and *Tl* Fd I) from His6 through Cys9 is not detectable in our data. The β-turn D which appears in the crystallographic structure of *Dg* Fd II[12] at amino acid positions 35–38 corresponding to the 36–39 residue range in *Dd*N Fd I was not found.

The ^{1}H NMR study presented here shows that the [4Fe–4S] ferredoxin I from *D. desulfuricans* Norway in 50 mM phosphate buffer at pH 5.9 and 25 °C adopts globally the same fold as other monocluster-type mesophilic ferredoxins from *Desulfovibrio* and reveals only minor differences from hyperthermostable ferredoxins.

Tertiary structure

Some long-range NOEs were observed in the ^{1}H NMR data, obtained with short mixing times, between the cluster and the secondary structural elements. For example, the αHCys15 (**III**) exhibits NOE cross peaks to αHAla47 and βHAla47. This indicates that part of the α-helix B lies in the vicinity of the iron cluster (Fig. 5).

Moreover, the observed (weak αHVal22–HNThr35 and medium αHVal22–HNAla36) NOEs cross-peaks are consistent with the 3.7 and 3.2 Å distances from the analogous residues found in the crystal structure of *Dg* Fd II.[12] Such observed NOEs indicate a hydrogen bond between the NH of Thr35 and the carbonyl of Val22 [Fig. 4(B)]. In addition, the buried character of the amide proton Thr35 is supported by the proton exchange data. The analysis of the NMR experiments in *Dd*N Fd I shows that the region ranging from Leu18 to

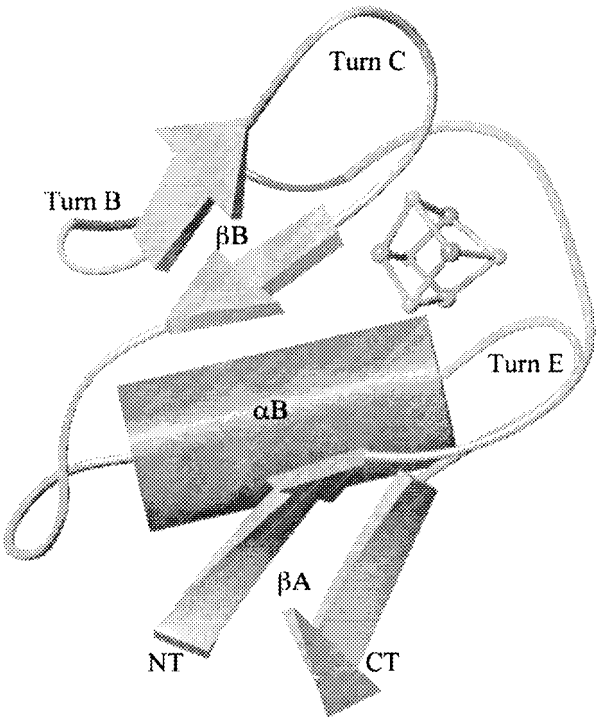

Figure 5. Schematic diagram of *Dd*N Fd I displaying α-helix B, β-sheets A and B and turns. NT and CT represent *N*- and *C*-terminus, respectively. The labeling of the secondary structure elements corresponds to that in Fig. 3.

Ala36 is buried and also highly structured, comprising one β-sheet (βB) and two turns (B and C) [Figs 3(A) and 4(B)]. This region is also in the close neighbourhood of the α-helix B. In fact, long range NOEs between βHLeu18–HNCys43 and γHLeu18–βHCys43 were indeed observed; they suggest the possible presence of a disulfide bridge. Analogous tertiary NOEs were found in 4 Fe *Tl* Fd (with NOE cross peaks at equivalent positions, i.e. between δHIle19 and βHCys43).

In order to examine the existence of such a disulfide bridge at 298 K in *Dd*N Fd I, we carried out a ^{13}C–^{1}H HSQC experiment at natural abundance on this ferredoxin. These experiments are based on work published by Chandrasekhar *et al.*[51] on the reduced and oxidized forms from the *Escherichia coli* thioredoxin.

This paper illustrates that $^{13}C_{\beta}$ chemical shifts for cysteines differ markedly between the disulfide and thiol states. For example, in the reduced thioredoxin, the $^{13}C_{\beta}$ of Cys32 and Cys35 chemical shift values are 24.3 and 25.9 ppm, respectively, to be compared with the corresponding downfield shifted values of 41.9 and 32.9 ppm in the disulfide state. The ^{13}C chemical shift values found in the ^{13}C–^{1}H HSQC experiment for ββ′HCys19 and ββ′HCys43 were found to be 34.6 and 32.2 ppm, respectively. These values, comparable to those of the oxidized thioredoxin, are more characteristic of a disulfide bond; they strengthen the observations made in ^{1}H NMR experiments.

The participation of a disulfide group in the redox

Table 2. Comparison of chemical shift values of the Leu18 to Phe23 segment in *Dd*N Fd I with equivalent data for 4Fe *Tl* Fd, 3Fe *Pf* Fd and *Tm* Fd

	*Dd*N Fd (298 K pH 5.9)	4Fe *Tl* Fd (303 K pH 7.5)	3Fe *Pf* Fd (303 K pH 7.0–8.0)	*Tm* Fd (303 K pH 6.0)
	Leu18	Ile19	Leu20	Leu19
NH	7.92	8.01	8.34	7.99
αH	4.15	4.01	4.19	4.19
	Cys19	Cys20	Cys21	Cys20
NH	8.11	8.15	7.90	8.13
αH	5.49	5.51	5.18	5.39
ββ′H	3.41/2.64	3.46/2.71	3.17/2.95	3.44/2.64
	Pro20	Pro21	Pro22	Pro21
αH	5.09	5.13	4.95	5.14
ββ′H	2.64/2.15	2.65/2.06	3.17/2.95	2.70/2.14
	Val22	Val23	Val24	Val23
NH	7.62	7.68	7.63	7.60
αH	3.93	3.84	3.91	3.71
ββ′H	1.30	1.29	1.43	1.48
γγ′H	0.69/ − 0.02	0.64/ − 0.13	0.76/ − 0.05	0.72/0.00
	Phe23	Phe24	Phe25	Phe24
NH	7.38	7.92	7.91	7.82
αH	5.54	5.52	5.03	5.46
ββ′H	3.04/2.33	2.85/2.24	2.78/2.30	2.89/2.31

cycle for an iron–sulfur cluster protein was proposed for both 3Fe *Pf* Fd and *Dg* Fd II. It is noted that *Dd*N Fd I, like *Dg* Fd, *Pf* Fd and *Tl* Fd, possesses Cys (**V**) and Cys (**VI**) opposite to the cluster, capable of forming a disulfide bridge. Our ^{1}H NMR and ^{13}C NMR data strongly support the presence of such a disulfide bridge between the two non-ligating Cys residues [Cys19 (**V**) and Cys43 (**VI**)] at the *N*-terminus of the α-helix B in *Dd*N Fd I. The pair formed by Cys19 and Cys43 present in *Dd*N Fd I is homologous with that participating in the disulfide bridge in *Dg* Fd II.[12]

A comparison of the chemical shift values of *Dd*N Fd I with those of other oxidized monocluster-type ferredoxins 4Fe *Tl* Fd, 3Fe *Pf* Fd[52] and *Thermotoga maritima* ferredoxin (*Tm* Fd)[32] reveals striking similarities located in a hydrophobic region ranging from Leu18 to Phe23 (Table 2). Indeed, in *Dg* Fd II, *Da* Fd I and *Bt* Fd ferredoxins the residues Leu18, Cys19, Pro20, Val22 and Phe23 were found to have a minimal water access surface (see Experimental).

It is of particular interest to note that the disulfide bridge, previously suggested, originates from Cys19. This fact therefore demonstrates that the reported high conservation of the 3D structure in the vicinity of the cluster, illustrated by striking similarities among the chemical shifts of the cysteine β-CH_2 protons of several oxidized 4Fe ferredoxins,[33] extends to the vicinity of the disulfide bridge. Such a conservation of the local 3D structure corroborates the idea of a role of the disulfide bridge in the redox process[36] in addition to the Fe–S cluster.

Acknowledgements

I gratefully acknowledge Dr O. Bornet for excellent NMR technical assistance. I thank Dr E. Loret and Dr W. Nitschke for critical reading of the manuscript and Dr F. Guerlesquin for the generous gift of ferredoxin (*Dd*N Fd I) and for comments on the manuscript.

REFERENCES

1. R. Cammack, *Adv. Inorg. Chem.* **38**, 281 (1992).
2. I. Bertini, S. Ciurli and C. Luchinat, *Struct. Bonding* (*Berlin*) **83**, 1 (1995).
3. M. M. Benning, T. E. Meyer, I. Rayment and H. M. Holden, *Biochemistry* **33**, 2476 (1994).
4. R. P. Sheridan, L. C. Allen and C. W. Carter, *J. Biol. Chem.* **256**, 5052 (1981).
5. J. L. Markley, T. M. Chan, R. Krishnamoorthi and E. Ulrich, in *Iron–Sulfur Protein Research*, edited by H. Matsubara, Y. Katsube and K. Wada, p. 167. Springer, New York (1986).
6. J. G. Huber, J. Gaillard and J. N. Moulis, *Biochemistry* **34**, 194 (1995).
7. M. Bruschi and F. Guerlesquin, *FEMS Microbiol. Rev.* **54**, 155 (1988).
8. E. T. Adman, L. C. Sieker and L. H. Jensen, *J. Biol. Chem.* **251**, 3801 (1976).
9. C. D. Stout, *J. Mol. Biol.* **205**, 545 (1989).
10. K. Fukuyama, H. Matsubara, T. Tsukihara and Y. Katsube, *J. Mol. Biol.* **210**, 383 (1989).
11. E. D. Due, E. Fanchon, J. Vicat, L. C. Sieker, J. Meyer and J.-M. Moulis, *J. Mol. Biol.* **243**, 683 (1994).
12. C. R. Kissinger, L. C. Sieker, E. T. Adman and L. H. Jensen, *J. Mol. Biol.* **219**, 693 (1991).
13. A. Séry, D. Housset, L. Serre, J. Bonicel, C. Hatchikian, M. Frey and M. Roth, *Biochemistry* **33**, 15408 (1994).
14. Z. Dauter, K. S. Wilson, L. C. Sieker, J. Meyer and J. M. Moulis, *Biochemistry* **51**, 16065 (1997).
15. J. M. Moulis, L. C. Sieker, K. S. Wilson and Z. Dauter, *Protein Sci.* **5**, 1765 (1996).
16. I. Bertini, A. Donaire, B. A. Feinberg, C. Luchinat, M. Piccioli and H. Yuan, *Eur. J. Biochem.* **232**, 192 (1995).
17. I. Bertini, A. Dikiy, D. H. W. Kastrau, C. Luchinat and P. Sompornpisut, *Biochemistry* **34**, 9851 (1995).
18. I. Bertini, M. M. J. Couture, A. Donaire, L. D. Eltis, I. C. Felli, C. Luchinat, M. Piccioli and A. Rosata, *Eur. J. Biochem.* **241**, 440 (1996).
19. I. Bertini, C. Luchinat and A. Rosata, *Prog. Biophys. Mol. Biol.* **66**, 43 (1996).
20. D. Bentrop, I. Bertini, F. Capozzi, A. Dikiy, L. Eltis and C. Luchinat, *Biochemistry* **35**, 5928 (1996).
21. L. S. Davy, M. J. Osborne and G. R. Moore, *J. Mol. Biol.* **277**, 683 (1998).
22. W. Fu, J. Telser, B. M. Hoffman, E. T. Smith, M. W. W. Adams, M. G. Finnegan, R. C. Conover and M. K. Johnson, *J. Am. Chem. Soc.* **116**, 5722 (1994).
23. L. Banci, I. Bertini and C. Luchinat, *Methods Enzymol.* **239**, 485 (1994).
24. C. Luchinat and M. Piccioli, in *NMR of Paramagnetic Macromolecules*, edited by G. N. La Mar, p. 7. NATO ASI Series, Kluwer, Dordrecht (1995).
25. G. N. La Mar and J. S. de Ropp, in *Biological Magnetic Resonance*, edited by L. J. Berliner and J. Reuben, Vol. 12, p. 1. Plenum Press, New York (1993).
26. M. J. Osborne, D. Crowe, S. L. Davy, C. MacDonald and G. R. Moore, *Methods Mol. Biol.* **60**, 233 (1997).
27. S. C. Busse, G. N. La Mar, L. P. Yu, J. B. Howard, E. T. Smith, Z. H. Zhou and M. W. W. Adams, *Biochemistry* **31**, 11952 (1992).
28. A. Donaire, C. M. Gorst, Z. H. Zhou, M. W. W. Adams and G. N. La Mar, *J. Am. Chem. Soc.* **116**, 6841 (1994).
29. A. Donaire, Z. H. Zhou, M. W. W. Adams and G. N. La Mar, *J. Biomol. NMR* **7**, 35 (1996).
30. Q. Teng, Z. H. Zhou, E. T. Smith, S. C. Busse, J. B. Howard, M. W. W. Adams and G. N. La Mar, *Biochemistry* **33**, 6316 (1994).
31. S. L. Davy, M. J. Osborne, J. Breton, G. R. Moore, A. J. Thomson, I. Bertini and C. Luchinat, *FEBS Lett.* **363**, 199 (1995).
32. G. Wildegger, D. Bentrop, A. Ejchart, M. Alber, A. Hage, R. Sterner and P. Rösch, *Eur. J. Biochem.* **229**, 658 (1995).
33. E. Lebrun, C. Simenel, F. Guerlesquin and M. Delepierre, *Magn. Reson. Chem.* **34**, 873 (1996).
34. D. Bentrop, I. Bertini, C. Luchinat, J. Mendes, M. Piccioli and M. Teixeira, *Eur. J. Biochem.* **236**, 92 (1996).
35. P. L. Wang, A. Donaire, Z. H. Zhou, M. W. W. Adams and G. N. La Mar, *Biochemistry* **35**, 11319 (1996).
36. C. M. Gorst, Z. H. Zhou, K. Ma, Q. Teng, J. B. Howard, M. W. W. Adams and G. N. La Mar, *Biochemistry* **34**, 8788 (1995).
37. D. Marion and F. Guerlesquin, *Biochem. Biophys. Res. Commun.* **159**, 592 (1989).
38. F. Guerlesquin, M. Bruschi, G. Bovier-Lapierre and G. Fauque, *Biochim. Biophys. Acta* **626**, 127 (1980).
39. A. Bax and D. G. Davis, *J. Magn. Reson.* **63**, 207 (1985).
40. A. Derome and M. Williamson, *J. Magn. Reson.* **88**, 177 (1990).
41. A. Kumar, R. R. Ernst, K. Wüthrich, *Biochem. Biophys. Res. Commun.* **95**, 7 (1981).
42. G. Bodenhauser and D. J. Ruben, *Chem. Phys. Lett.* **69**, 185 (1980).
43. A. Bax, M. Ikura, L. E. Kay, D. A. Torchia and R. Tschudin, *J. Magn. Reson.* **86**, 304 (1990).
44. A. J. Shoka, P. B. Barker and R. Freeman, *J. Magn. Reson.* **64**, 547 (1985).
45. K. Wüthrich, *NMR of Proteins and Nucleic Acids.* Wiley, New York (1986).
46. G. M. Clore, A. J. Brünger, M. Karplus and A. M. Gronenborn, *J. Mol. Biol.* **191**, 523 (1986).
47. A. T. Brünger, *X-PLOR, Version 3.1.* Yale University Press, New Haven, CT (1993).
48. L. Banci, I. Bertini, P. Carloni, C. Luchinat and P. L. Orioli, *J. Am. Chem. Soc.* **114**, 7683 (1992).
49. W. Kabsch and C. Sander, *Biopolymers* **22**, 2577 (1983).
50. D. S. Wishart, B. D. Sykes and F. M. Richards, *J. Mol. Biol.* **222**, 311 (1991).
51. K. Chandrasekhar, A. P. Campbell, M. F. Jeng, A. Holmgreen and H. J. Dyson, *J. Biomol. NMR* **4**, 411 (1994).
52. C. M. Gorst, Y. H. Yeh, Q. Teng, L. Calzolai, Z. H. Zhou, M. W. W. Adams and G. N. La Mar, *Biochemistry* **34**, 600 (1995).

